Am J Transl Res 2021;13(1):286-300
www.ajtr.org /ISSN:1943-8141/AJTR0118946

Original Article

CARD11 alteration as a candidate biomarker of skin cutaneous melanoma treated with immune checkpoint blockade

Yutian Si[1,2*], Anqi Lin[1*], Weimin Ding[1*], Hui Meng[1], Peng Luo[1], Jian Zhang[1]

[1]Department of Oncology, Zhujiang Hospital, Southern Medical University, Guangzhou 510282, China; [2]Southern Medical University, Guangzhou 510282, China. [*]Equal contributors.

Received July 26, 2020; Accepted November 24, 2020; Epub January 15, 2021; Published January 30, 2021

Abstract: Background: Immune checkpoint inhibitors (ICIs) can be problematic, including a lack of sustained clinical response, in the treatment of skin cutaneous melanoma (SKCM) patients; therefore, predictive biomarkers are urgently needed. Recently, gene mutations identified by melanoma genomic analysis have shown great predictive potential. Methods: We collected an immunotherapy cohort and The Cancer Genome Atlas (TCGA)-SKCM cohort from published studies and tested the predictive function of the CARD11 mutation. We then further studied the association between the CARD11 mutation and tumor immunogenicity by studying related genes and pathways in the tumor microenvironment (TME). Results: In the immunotherapy and TCGA-SKCM cohorts, patients with CARD11-mutant (MT) tumors had longer overall survival (OS) and a better prognosis than those with CARD11-wild-type (WT) tumors. CARD11-MT tumors had higher immunogenicity, and gene expression related to immunosuppression was significantly downregulated in CARD11-MT tumors. We found that immunosuppression-related pathways were significantly downregulated in CARD11-MT tumors, while immune activation-related pathways were significantly upregulated. Additionally, CARD11-MT tumors had more DNA damage response and repair (DDR) pathway mutations. Conclusions: CARD11 mutation is associated with longer OS and a better prognosis after ICI treatment. Therefore, the CARD11 gene can be used as a biomarker for predicting the efficacy of ICIs in SKCM patients.

Keywords: CARD11, immune checkpoint inhibitors, skin cutaneous melanoma, biomarker, prognosis

Introduction

Skin cutaneous melanoma (SKCM) is an extremely aggressive malignancy, with approximately 200,000 new cases diagnosed each year worldwide [1]. The 5-year overall survival (OS) rate of patients with advanced melanoma is only 10-29%, and the overall response rate (ORR) of traditional chemotherapy is less than 20%. BRAF inhibitors, interleukin (IL)-2, adoptive T cell therapy, etc. are not widely used clinically due to adverse reactions or poor efficacy [2, 3]. In contrast, immunotherapy, especially immune checkpoint inhibitors (ICIs), can significantly prolong OS and improve patient prognosis. However, in clinical practice, only a few patients have achieved a lasting response with ICIs. As a consequence, to reduce adverse reactions and the cost of treatment, reliable predictive biomarkers are needed to guide the clinical diagnosis and treatment processes.

At present, predictive markers for immunotherapy in melanoma include lactate dehydrogenase (LDH), tumor-infiltrating lymphocytes (TILs), PD-L1 expression, and the tumor mutational burden (TMB), among others, but these markers are not sufficient for predicting outcomes. In addition, melanoma genomics-based gene mutation research is a popular approach for biomarker discovery. For example, NRAS (10-25%) and NF1 (14%) are commonly mutated in melanoma, and some studies have shown that patients with NRAS mutations have a higher response rate (28% vs. 16%, P = 0.04) to first-line immunotherapy with IL-2, ipilimumab or an anti-PD-L1 antibody than patients with wild-type NRAS [4]. Moreover, NF1-mutant melanoma is associated with UV damage, a high TMB, and a high response rate to anti-PD-1 immunotherapy [5]. These results suggest that certain gene mutations can predict the therapeutic effect of immunotherapy and may be reli-

able predictive markers of immunotherapeutic efficacy.

Caspase Recruitment Domain Family Member 11 (CARD11) is a protein-coding gene whose product transmits an essential costimulatory signal for T cell activation mediated by T cell receptors (TCRs) that plays important roles in NF-κB activation and lymphocyte signaling [6]. Recent studies have shown that CARD11-BCL10-MALT1 (CBM) signaling can mediate TCR-induced NF-κB activation in regulatory T cells (Tregs) and control the conversion of resting Tregs into effector Tregs under steady-state conditions. Selective inhibition of BCL10 signaling in Tregs can enhance the body's antitumor response in a mouse melanoma model [7]. This suggests that changes in the CARD11 gene and its pathway can affect antitumor immunity by affecting the function of infiltrating T cells and the content of related cytokines in the tumor immune microenvironment, thus improving or worsening the prognosis of patients.

In this article, we analyzed CARD11-related genes and pathways in the tumor immune microenvironment in an SKCM immunotherapy cohort and The Cancer Genome Atlas (TCGA)-SKCM cohort and explored the feasibility and validity of the following hypothesis: CARD11 gene mutation may be a good independent predictive marker of SKCM outcomes, which may help to identify patients with a relatively good response and prognosis after ICI treatment.

Methods

Acquisition and screening of clinical data

First, we used an immunotherapy cohort (reported by Rizvi et al. [8]) containing clinical data and targeted sequencing (Panel) data to assess whether CARD11 mutations could predict the prognosis of SKCM patients treated with ICIs. Based on their CARD11 gene status, SKCM patients (n = 183) with CARD11 gene mutation data in the immunotherapy cohort (anti-CTLA-4 and anti-PD-1/PD-L1 therapies; 146 anti-CTLA-4 antibody-treated patients, 1,256 anti-PD-1 or anti-PD-L1 antibody-treated patients, and 260 combination therapy patients) were divided into CARD11-mutant (MT) and CARD11-wild-type (WT) groups. Kaplan-Meier (KM) analysis was used for survival analysis. We screened the data of CANCER TYPE = "melanoma" & histology = "cutaneous" (n = 187) for analysis. Additionally, we downloaded the somatic mutation data and OS data for the cohort TCGA-SKCM from the Genomic Data Commons (https://portal.gdc.cancer.gov/) using the R package TCGAbiolinks [9]. We used cBioportal [10] to download the disease-free survival (DFS) data of the patients in the cohort TCGA-SKCM and used the KM method to analyze survival for different groups in the cohort TCGA-SKCM.

Tumor immunogenicity analysis and identification of CARD11 gene mutation characteristics

First, we obtained and screened the somatic mutation data (reported by Rizvi et al.) of 183 SKCM samples from the immunotherapy cohort generated by targeted next-generation sequencing (NGS; MSK-IMPACT) for the purpose of tumor immunogenicity analysis. In a previous study, Thorsson V et al. [11] reported data on the neoantigen load (NAL) for the cohort TCGA-SKCM. Whole-exome sequencing (WES) data for SKCM cell line analysis were downloaded from Genomics of Drug Sensitivity in Cancer (GDSC) [12]. Consistent with reports from related articles [13], the method that we used to quantify the TMB in the SKCM immunotherapy cohort (Rizvi et al.), TCGA-SKCM cohort and GDSC-SKCM cohort used nonsynonymous MTations in these cohorts as the raw MTation count, which was divided by 38 Mb. Next, we described the mutation characteristics of the CARD11 gene using R software. The visual analytics of the top 20 genes with the highest mutation frequencies and related clinical features in the immunotherapy cohort and TCGA-SKCM cohort were performed using the R package ComplexHeatmap [14]. The visual analytics of CARD11 mutation sites in the immunotherapy cohort and TCGA-SKCM cohort were performed using the R package Maftools [15].

Identification of tumor immune microenvironment characteristics and drug sensitivity analysis of tumor cells

The gene expression data (Illumina HiSeq, RNA-Seq) used to analyze TCGA-SKCM tumor immune microenvironment characteristics were obtained from TCGAbiolinks, and we also performed CIBERSORT [16] (http://cibersort.stanford.edu/) analysis to compare the differences in infiltrating immune cells between CARD11-

WT and CARD11-MT tumors. In addition, we compared and analyzed the mRNA expression levels of immune-related genes in TCGA-SKCM. Specifically, we extracted immune cell marker genes from a previously published study by Hao D et al. [17]. In addition, we also used the method of immune gene functional classification previously reported by Thorsson et al. [11] to classify immune-related genes and used the log2 (FPKM + 1) method to quantify the expression of these genes. The cut-off value of logFC was ± 1. In a susceptibility analysis of SKCM tumor cells, we downloaded SKCM cell line drug sensitivity data from GDSC and then compared the sensitivities of CARD11-WT and CARD11-MT tumors.

Copy number alteration (CNV) analysis

When analyzing copy number variations in the CARD11 gene, we used Broad GDAC Firehose (http://gdac.broadinstitute.org/) to download TCGA-SKCM's Affymetrix SNP arrays 6.0 data (hg19; germline/potential false-positive calls removed), and then GISTIC 2.0 analysis was performed on the obtained CNV segments using GenePattern 2.0[18] (https://cloud.genepattern.org/gp/pages/index.jsf). In the process of GISTIC 2.0 analysis, except for individual parameters that were specific (such as the confidence level set to 0.99; X-chromosome may be included before analysis), the parameters were set to the default parameters. Finally, we used the R package Maftools [15] to visualize the CNV, which was the result of the GISTIC 2.0 analysis.

Analysis of gene set pathway enrichment and the DNA damage response and repair (DDR) pathway

The gene expression data (raw count) required for pathway enrichment analysis were normalized and subsequently analyzed using the R package edgeR [19]. Next, we used the clusterProfiler R package [20] for gene annotation enrichment analysis. It should be emphasized that in Gene Ontology (GO), Kyoto Encyclopedia of Genes and Genomes (KEGG) and Reactome analyses, statistical significance was defined as $P < 0.05$. In addition, to evaluate the number of nonsynonymous mutations in DDR pathway components in the immunotherapy cohort and TCGA-SKCM cohort, we downloaded the gene set related to the DDR pathways in the MSigDB database of Broad Institute [21] (Additional File: Table S1). Then, we completed the evaluation using this DDR gene set. Additionally, we compared the difference between CARD11-WT tumors and CARD11-MT tumors in regard to the number of nonsynonymous mutations in the DDR pathway.

Statistical analysis

We used the Mann-Whitney U test to compare and analyze the TMB, NAL, immune cell content, immune-related gene expression, age, microsatellite instability (MSI) score, and number of DDR pathway mutations in CARD11-WT and CARD11-MT tumors. Fisher's exact test was used to analyze CARD11-WT and CARD11-MT tumors for differences in the top 20 gene mutation rates, sex and immunotherapy responses in the immunotherapy cohort. Additionally, the differences between CARD11-WT and CARD11-MT tumors in terms of the gene mutation status for the top 20 mutation rates in the cohort TCGA-SKCM were also determined. Fisher's exact test was used to compare the differences in sex, race, ethnicity, and clinical stage between CARD11-WT and CARD11-MT patients in TCGA-SKCM. The KM method and log-rank test were used to analyze the progression-free survival and OS of patients with CARD11-MT or CARD11-WT tumors. In our data analysis, statistical significance was defined as $P < 0.05$, and all statistical analyses were performed using a two-sided test. Finally, we used R software (version 3.6.1) to test all the statistical results and completed the visualization. In the process of visual analysis, we used the R package ggpurb to draw boxplots [22]. The false discovery rate (FDR) of the CNV visualization was defined as 0.05.

Results

Associations between the CARD11 status and clinical characteristics of patients

In the SKCM immunotherapy cohort, a total of 183 patients were obtained after data filtering, of which 26 patients had mutations in the CARD11 gene (CARD11-MT), and the remaining 157 patients did not have mutations (CARD11-WT). As hypothesized, the CARD11-MT patients had a better prognosis after immunotherapy than the CARD11-WT patients (**Figure 1A**, $P = 0.026$, hazard ratio (HR) = 0.29, 95% confidence interval (CI): 0.15-0.59). In addition, we performed a survival analysis on the cohort of

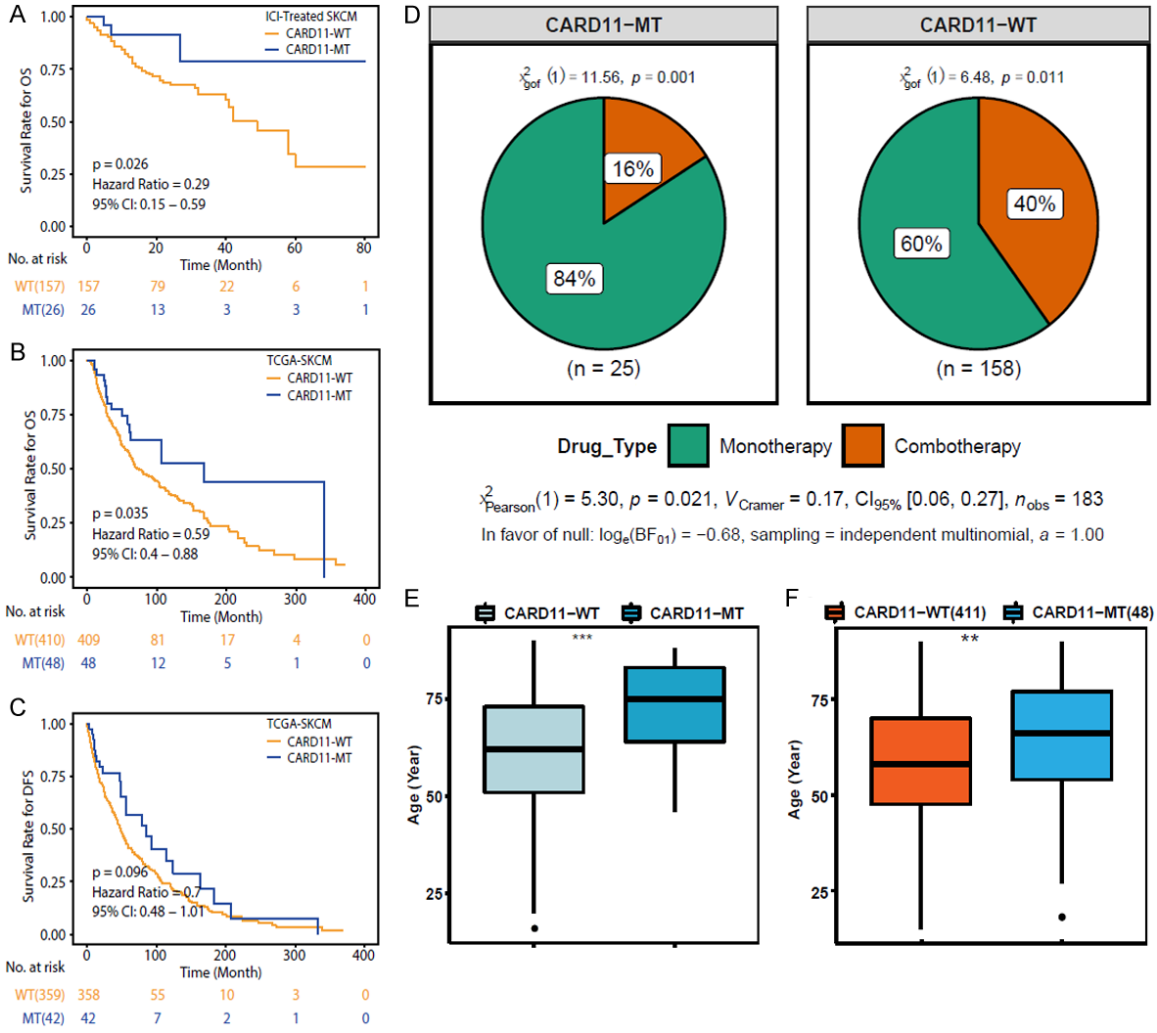

Figure 1. Associations between the CARD11 gene status and patient clinical characteristics. (A) Kaplan-Meier analysis was used to compare the overall survival (OS) of CARD11-MT patients with that of CARD11-WT patients in the ICI treatment cohort (N = 183). (B) Kaplan-Meier analysis was used to compare the overall survival (OS) of CARD11-MT patients with that of CARD11-WT patients in the cohort TCGA-SKCM (N = 457). (C) Kaplan-Meier analysis was used to compare the disease-free survival (DFS) of CARD11-MT patients with that of CARD11-WT patients in the cohort TCGA-SKCM (N = 400). (D) The pie chart shows the drug types used in the cohort TCGA-SKCM. The CARD11 gene status was obtained from MSKCC; n (CARD11-MT) = 25, n (CARD11-WT) = 158. Green: monotherapy, orange: combination therapy. (E, F) The Mann-Whitney U test was used to compare the ages of CARD11-WT and CARD11-MT patients. The data were obtained from the MSKCC (E) and TCGA (F) databases. *P < 0.05; **P < 0.01; ***P < 0.001.

SKCM patients without immunotherapy in TCGA and found that the CARD11-MT patients had better OS than the CARD11-WT patients (**Figure 1B**, P = 0.035, HR = 0.59, 95% CI = 0.4-0.88). There was no significant difference in DFS (**Figure 1C**). To better describe the clinical characteristics of CARD11-MT patients, we performed a clinical variable test. In the SKCM cohort, there were 25 CARD11-MT patients and 158 CARD11-WT patients. Most of these patients received monotherapy (**Figure 1D**), but the CARD11-WT patients were more likely to be treated with combination therapy. In addition, we analyzed the differences in patient age between the CARD11-MT and CARD11-WT patients. In the cohort TCGA-SKCM and immunotherapy cohort, the CARD11-MT patients were older, and the difference was statistically significant (**Figure 1E**, **1F**). Finally, Figure S1 shows the statistically significant differences between CARD11-MT and CARD11-WT tumor cells in the GDSC database. It is worth noting that for

FH535 (a Wnt/β-catenin and PPAR inhibitor) and tipifarnib (a CXCL12/CXCR4 pathway inhibitor), the CARD11-MT cell line was more resistant than the CARD11-WT cell line.

Characteristics of CARD11 gene mutation

To understand the effect of CARD11 gene mutation at the gene level, we performed a CNV analysis. The most obvious changes in CARD11-MT patients were the expansion of the 3p13 site, deletion of the 2q37.3 site, and disappearance of 11q13.3 site amplification (**Figure 2A**). To further explore the influence of mutations on CARD11 gene function, we performed a visual analysis and found that mutation sites appeared in the CARD11-like protein-coding region, the BAR domain, the PDZ domain, the SH3 domain superfamily, and the P-loop-nucleoside triphosphate hydrolase region and were especially predominant in the P-loop-nucleoside triphosphate hydrolase region and BAR domain (**Figure 2B**). Finally, to obtain a general understanding of the characteristics of CARD11 gene mutations, we plotted gene mutation panoramas for the SKCM immunotherapy cohort and TCGA-SKCM cohort separately, which showed significant differences between the CARD11-MT and CARD11-WT groups in clinical characteristics such as patient age, treatment, TMB, NAL, and prognosis (**Figure 2C**, **2D**). In both cohorts, the CARD11-MT patients were older and had a higher TMB. The most frequently occurring mutations in the CARD11 gene were missense mutations (96.3% and 94.1%). The difference between the two cohorts was that the CARD11-MT and CARD11-WT patients in the immunotherapy cohort had significant differences in the type of treatment, OS, and NF1 (mainly splice site mutation) and PTPRT (mainly missense mutation) gene mutations. Different groups of patients in the cohort from TCGA-SKCM had significant differences in sex and NAL, and there were also differences in mutations in DNAH5, PCLO, LRP1B, ADGRV1 and other genes (mainly missense mutations).

The CARD11-MT status is associated with relatively high tumor immunogenicity and a relatively strong antitumor effect

To characterize the tumor immune microenvironment of CARD11-MT tumors, we compared tumor immunogenicity and antitumor immunity between CARD11-MT and CARD11-WT tumors. In the SKCM immunotherapy cohort and TCGA-SKCM cohort, the TMB in the CARD11-MT tumors was significantly higher than that in the CARD11-WT tumors. Therefore, the NAL in the CARD11-MT tumors was also significantly higher (**Figure 3A**), suggesting that CARD11 mutation is associated with enhanced tumor immunogenicity. On the other hand, compared with CARD11-WT tumors, CARD11-MT tumors had a significant reduction in gene expression in cells that inhibit antitumor activity in the immune microenvironment, such as Tregs and myeloid-derived suppressor cells (MDSCs), while PROK2 gene expression in neutrophils was upregulated (**Figure 3B**). As shown in the cellular gene heatmap, we found that the expression levels of some genes in mast cells, such as SERPINB2, KRT1, and CMA1, were significantly downregulated in CARD11-MT tumors, while the expression levels of RGS16 genes were upregulated. In addition, we also observed a significant decrease in the expression of T cell genes, such as GAL, EPHA4, and IL1B, in the TME. To better characterize immunological characteristics, we thoroughly examined the differences in immune-related gene expression levels between CARD11-MT and CARD11-WT tumors (**Figure 3C**). Consistent with the heatmap of immune cell genes, the expression of suppressive immunoregulatory genes, such as ARG1, in CARD11-MT tumors was usually downregulated (**Figure 3C**), and the expression of certain genes that activate receptors that participate in antitumor signaling, such as TNFRSF14, was upregulated. In CARD11-MT tumors, the gene expression of certain antigen-presenting factors, such as HLA-DRB1, was also upregulated.

Pathway analysis related to CARD11-MT disease

Gene set enrichment analysis (GSEA) reveals CARD11-MT tumor-related pathways: By GSEA, we found that some pathways were enriched in CARD11-MT tumors. Changes in these pathways may explain why CARD11-MT patients have a better prognosis than CARD11-WT patients after immunotherapy at the molecular level. Some pathways that promote tumor progression were downregulated in CARD11-MT tumors, which may be one of the reasons for the improved prognosis. Fatty acid metabolism

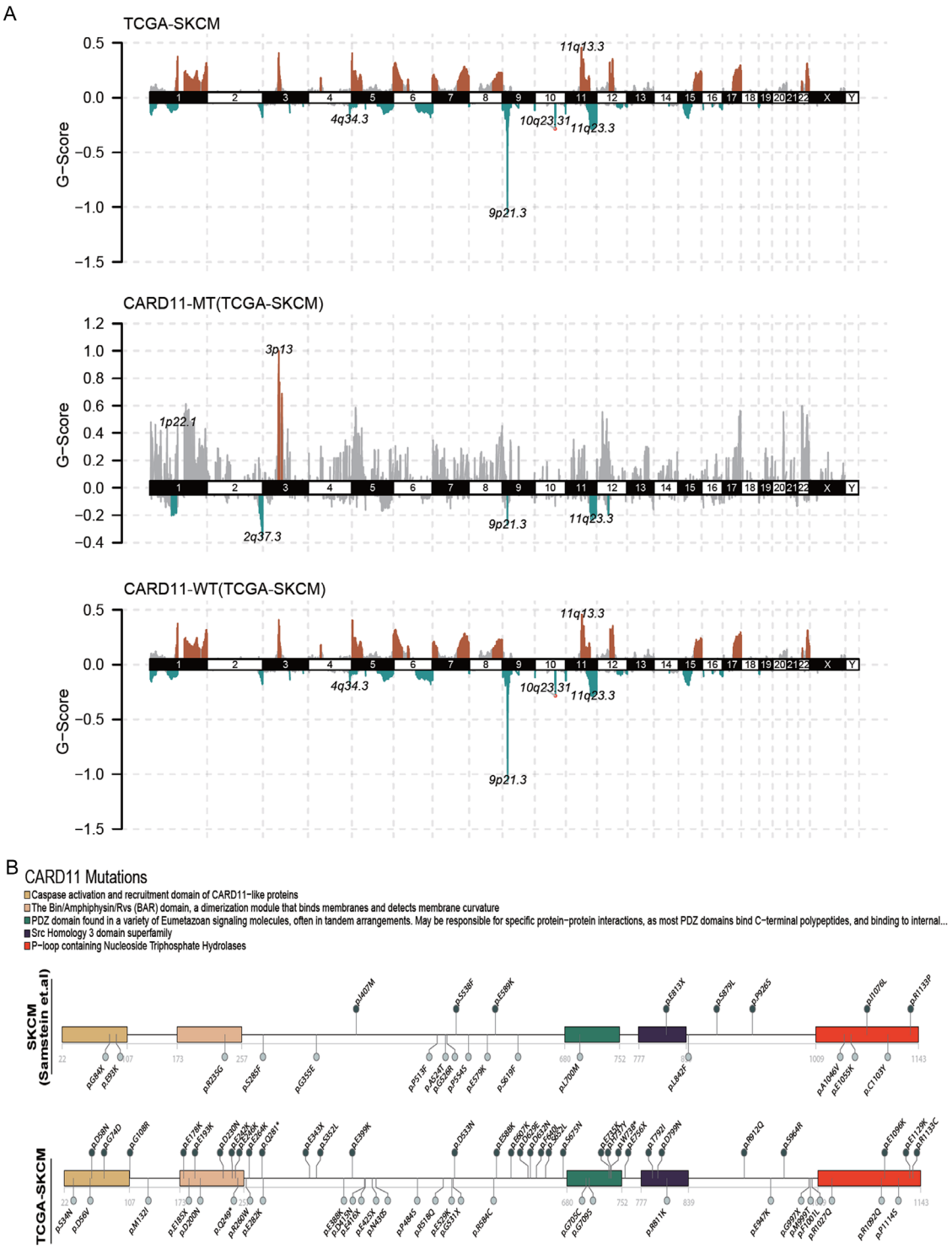
A
TCGA-SKCM
G-Score
11q13.3
4q34.3
10q23.31
11q23.3
9p21.3
CARD11-MT(TCGA-SKCM)
3p13
1p22.1
2q37.3
CARD11-WT(TCGA-SKCM)
B
CARD11 Mutations
Caspase activation and recruitment domain of CARD11-like proteins
The Bin/Amphiphysin/Rvs (BAR) domain, a dimerization module that binds membranes and detects membrane curvature
PDZ domain found in a variety of Eumetazoan signaling molecules, often in tandem arrangements. May be responsible for specific protein-protein interactions, as most PDZ domains bind C-terminal polypeptides, and binding to internal...
Src Homology 3 domain superfamily
P-loop containing Nucleoside Triphosphate Hydrolases
SKCM (Samstein et.al)
TCGA-SKCM

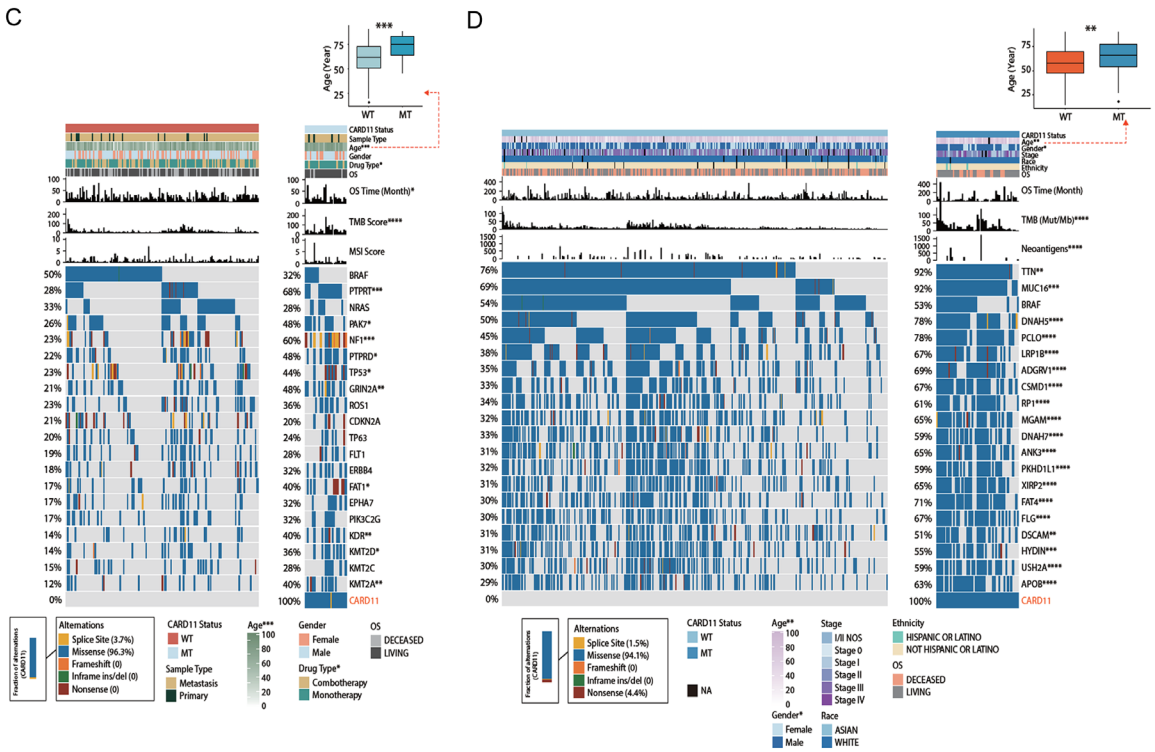

Figure 2. Characteristics of CARD11 gene mutations. A. Copy number variation analysis of the CARD11 gene. Top: CARD11 copy number variation in the cohort TCGA-SKCM. Middle: CARD11-MT copy number variation in the cohort TCGA-SKCM. Bottom: CARD11-WT copy number variation in the cohort TCGA-SKCM. Red: copy number increased, green: copy number decreased. B. Visual analysis of CARD11 gene mutations. CARD11 mutation data were obtained from the data in Samstein et al. (top) and from the cohort TCGA-SKCM (bottom). Yellow: CARD11-like protein-coding region, orange: BAR domain, green: PDZ domain, purple: SH3 domain superfamily, red: P-loop-nucleoside triphosphate hydrolase region. C. Panorama of CARD11 mutations in the SKCM immunotherapy cohort. Mutation types: yellow: splice site; blue: missense; orange: frameshift; green: inframe ins/del; red: nonsense. The patient notes above show the CARD11 status, type (carcinoma in situ/metastatic cancer), age, sex, type of treatment, and OS of each patient. The middle histogram shows the OS, TMB score, and MSI score of each patient. The mutation frequency of each gene is shown on the left. D. Panorama of CARD11 gene mutations in the SKCM immunotherapy cohort. Mutation types: yellow: splice site; blue: missense; orange: frameshift; green: inframe ins/del; red: nonsense. The patient notes above show the CARD11 status, age, sex, clinical stage, race, ethnicity, and OS of each patient. The middle histogram shows the OS, TMB and NAL of each patient. The mutation frequency of each gene is shown on the left.

is important for tumor evolution and progression, and downregulation of these pathways may inhibit tumor growth (**Figure 4A**). The pathways that were upregulated in CARD11-MT tumors related to the promotion of antitumor immunity were mainly related to T cell activation (**Figure 4B**). In addition, GSEA of GDSC data revealed that some carcinogenic pathways, such as the RAS and MET pathways, were downregulated in CARD11-MT tumor cells (**Figure 4C**). In addition, the pathways that downregulate the G2/M transition of the cell cycle were enriched, suggesting that tumor cells may be arrested in the G2 phase when proliferating, which could lead to apoptosis (**Figure 4D**).

The number of mutations in the DDR pathway was significantly upregulated in CARD11-MT tumors: We analyzed the number of mutations in DDR pathway genes (SKCM immunotherapy cohort and TCGA-SKCM cohort, Additional File Table S1). In the immunotherapy cohort, we found that most of the DDR pathways (except FA) had more mutations in the CARD11-MT group than in the CARD11-WT group (**Figure 4E**). Similarly, in TCGA-SKCM, we found that the number of mutations in all DDR pathways in the CARD11-MT group was also higher than that in the CARD11-WT groups (**Figure 4F**). These results may be the reasons for the increased TMB and tumor immunogenicity of CARD11-MT tumors.

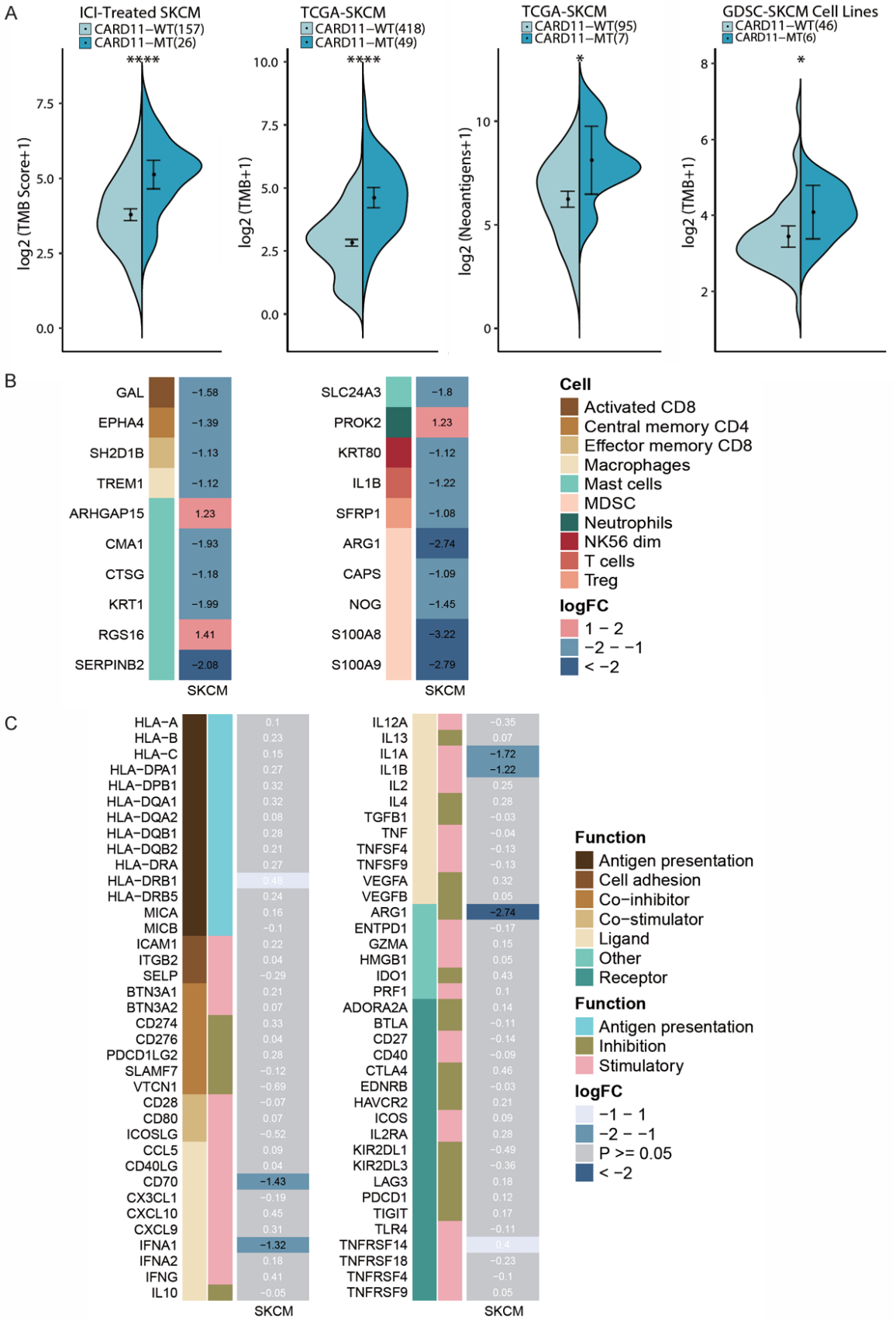
A
ICI-Treated SKCM
CARD11−WT(157)
CARD11−MT(26)
****
log2 (TMB Score+1)
TCGA-SKCM
CARD11−WT(418)
CARD11−MT(49)
****
log2 (TMB+1)
TCGA-SKCM
CARD11−WT(95)
CARD11−MT(7)
*
log2 (Neoantigens+1)
GDSC-SKCM Cell Lines
CARD11−WT(46)
CARD11−MT(6)
*
log2 (TMB+1)
B
GAL −1.58
EPHA4 −1.39
SH2D1B −1.13
TREM1 −1.12
ARHGAP15 1.23
CMA1 −1.93
CTSG −1.18
KRT1 −1.99
RGS16 1.41
SERPINB2 −2.08
SKCM
SLC24A3 −1.8
PROK2 1.23
KRT80 −1.12
IL1B −1.22
SFRP1 −1.08
ARG1 −2.74
CAPS −1.09
NOG −1.45
S100A8 −3.22
S100A9 −2.79
SKCM
Cell
Activated CD8
Central memory CD4
Effector memory CD8
Macrophages
Mast cells
MDSC
Neutrophils
NK56 dim
T cells
Treg
logFC
1 − 2
−2 − −1
< −2
C
HLA−A 0.1
HLA−B 0.23
HLA−C 0.15
HLA−DPA1 0.27
HLA−DPB1 0.32
HLA−DQA1 0.32
HLA−DQA2 0.08
HLA−DQB1 0.28
HLA−DQB2 0.21
HLA−DRA 0.27
HLA−DRB1 0.48
HLA−DRB5 0.24
MICA 0.16
MICB −0.1
ICAM1 0.22
ITGB2 0.04
SELP −0.29
BTN3A1 0.21
BTN3A2 0.07
CD274 0.33
CD276 0.04
PDCD1LG2 0.28
SLAMF7 −0.12
VTCN1 −0.69
CD28 −0.07
CD80 0.07
ICOSLG −0.52
CCL5 0.09
CD40LG 0.04
CD70 −1.43
CX3CL1 −0.19
CXCL10 0.45
CXCL9 0.31
IFNA1 −1.32
IFNA2 0.18
IFNG 0.41
IL10 −0.05
SKCM
IL12A −0.35
IL13 0.07
IL1A −1.72
IL1B −1.22
IL2 0.25
IL4 0.28
TGFB1 −0.03
TNF −0.04
TNFSF4 −0.13
TNFSF9 −0.13
VEGFA 0.32
VEGFB 0.05
ARG1 −2.74
ENTPD1 −0.17
GZMA 0.15
HMGB1 0.05
IDO1 0.43
PRF1 0.1
ADORA2A 0.14
BTLA −0.11
CD27 −0.14
CD40 −0.09
CTLA4 0.46
EDNRB −0.03
HAVCR2 0.21
ICOS 0.09
IL2RA 0.28
KIR2DL1 −0.49
KIR2DL3 −0.36
LAG3 0.18
PDCD1 0.12
TIGIT 0.17
TLR4 −0.11
TNFRSF14 0.4
TNFRSF18 −0.23
TNFRSF4 −0.1
TNFRSF9 0.05
SKCM
Function
Antigen presentation
Cell adhesion
Co−inhibitor
Co−stimulator
Ligand
Other
Receptor
Function
Antigen presentation
Inhibition
Stimulatory
logFC
−1 − 1
−2 − −1
P >= 0.05
< −2

Figure 3. Tumor immunogenicity and gene expression characteristics of CARD11-MT tumors. A. Comparison of the tumor mutational load between CARD11-MT and CARD11-WT tumors in the SKCM immunotherapy cohort, TCGA-SKCM cohort, and GDSC-SKCM cell line dataset. Comparison of the neoantigen load between CARD11-MT and CARD11-WT tumors in the cohort TCGA-SKCM. B. Heatmap depicting the average difference in the mRNA expression of immune cell marker genes between CARD11-MT and CARD11-WT SKCM tumors. The x-axis of the heatmap represents the cell type and logFC value, and the y-axis represents the name of the relevant cell line. Each square represents a fold change or difference in each indicated immune cell marker gene between the CARD11-MT and CARD11-WT SKCM tumors. Red represents gene upregulation, and blue represents gene downregulation. The cut-off value of logFC was ± 1. C. Heatmap depicting the average difference in the mRNA expression of immune-related genes between CARD11-MT and CARD11-WT SKCM tumors. The x-axis of the heatmap represents gene function and logFC values, and the y-axis represents the names of immune-related genes. Each square represents a fold change or difference in each of the indicated immune-related genes between CARD11-MT and CARD11-WT SKCM tumors. White: -1 <logFC <1; gray: $P \geq 0.05$; blue: gene expression was downregulated. The cut-off value of logFC was ± 1.

Discussion

In this study, we analyzed the immunotherapy and TCGA-SKCM cohorts we enrolled and found that CARD11 mutation could predict the response to immunotherapy in SKCM patients. By analyzing immune-related genes, CARD11-MT tumor-related pathways, DDR pathways and other factors in the tumor immune microenvironment, we have explained the reasons why CARD11-MT patients have a better prognosis than CARD11-WT patients initially after immunotherapy, and the relevant mechanisms will be discussed in detail in the following sections (**Figure 5**).

First, MDSC numbers and immunosuppressive pathway activity were significantly downregulated in CARD11-MT tumors. In CARD11-MT tumors, we found the downregulation of the expression of genes related to MDSCs, such as ARG1, S100A8, and S100A9, which are essential for MDSCs to perform immunosuppressive functions. It is known that the most important factor that enables MDSCs to perform immunosuppressive functions is the expression products of ARG1 [23]. Arginine hydrolase is an important product of ARG1 gene expression, which is secreted into the tumor immune microenvironment and acquired by CD8+ T cells. In T cells, arginine hydrolase can inhibit proliferation by consuming L-Arg, which is necessary for T cell activation, eventually leading to reduced T cell proliferation and T cell suppression [24]. Arginine hydrolase can also reduce the secretion of antitumor cytokines, such as IFN-γ, TNF-α, and IL-2 [24]. In addition, in the TME, the proteins encoded by the S100A8 and S100A9 genes have autocrine and paracrine functions, maintaining myeloid cell recruitment, immunosuppression and NF-κB signaling. The cytokines CXCL1 and CXCL2, which are released by primary tumors, also promote the recruitment of myeloid cells to maintain a proinflammatory environment and promote tumor metastasis [25]. The ARG1 and S100A8/9 genes are important genes for achieving MDSC function, and their downregulation will certainly downregulate MDSC function in the TME, which will eventually lead to the weakening of T cell inhibition and IFN-γ inhibition. Then, ICIs can exert their antitumor effects.

Second, when performing GSEA, we found that CARD11-MT tumors had significant downregulation of pathways related to fatty acid metabolism. As early as the 1950s, Medes et al. discovered that the fatty acids required for the growth and proliferation of malignant tumor cells are mainly derived from the de novo synthesis pathway [26]; a type of unsaturated fatty acid, arachidonic acid, is synthesized in tumor cells, and its metabolism closely related to the growth of tumor cells. In tumor cells, linoleic acid generates arachidonic acid via catalysis by dehydrogenase, and arachidonic acid is further catalyzed into prostaglandins, leukotrienes, and thromboxane (eicosanoids). Among these products, PEG2 is closely related to cancer development [27]. A large amount of PEG2 synthesized in tumor cells can be secreted into the microenvironment and induce immunosuppression in the following ways [28]: inhibiting the proliferation and activation of CD8+ T cells, inhibiting the antitumor activity of natural killer cells, stimulating the proliferation of Tregs and MDSCs, and inhibiting the differentiation of dendritic cells (DCs) and changing their functions to induce T cell tolerance. In addition to the metabolism of arachidonic acid, enzymes related to fatty acid metabolism in tumor cells, such as fatty acid synthase (FAS) and acetyl-

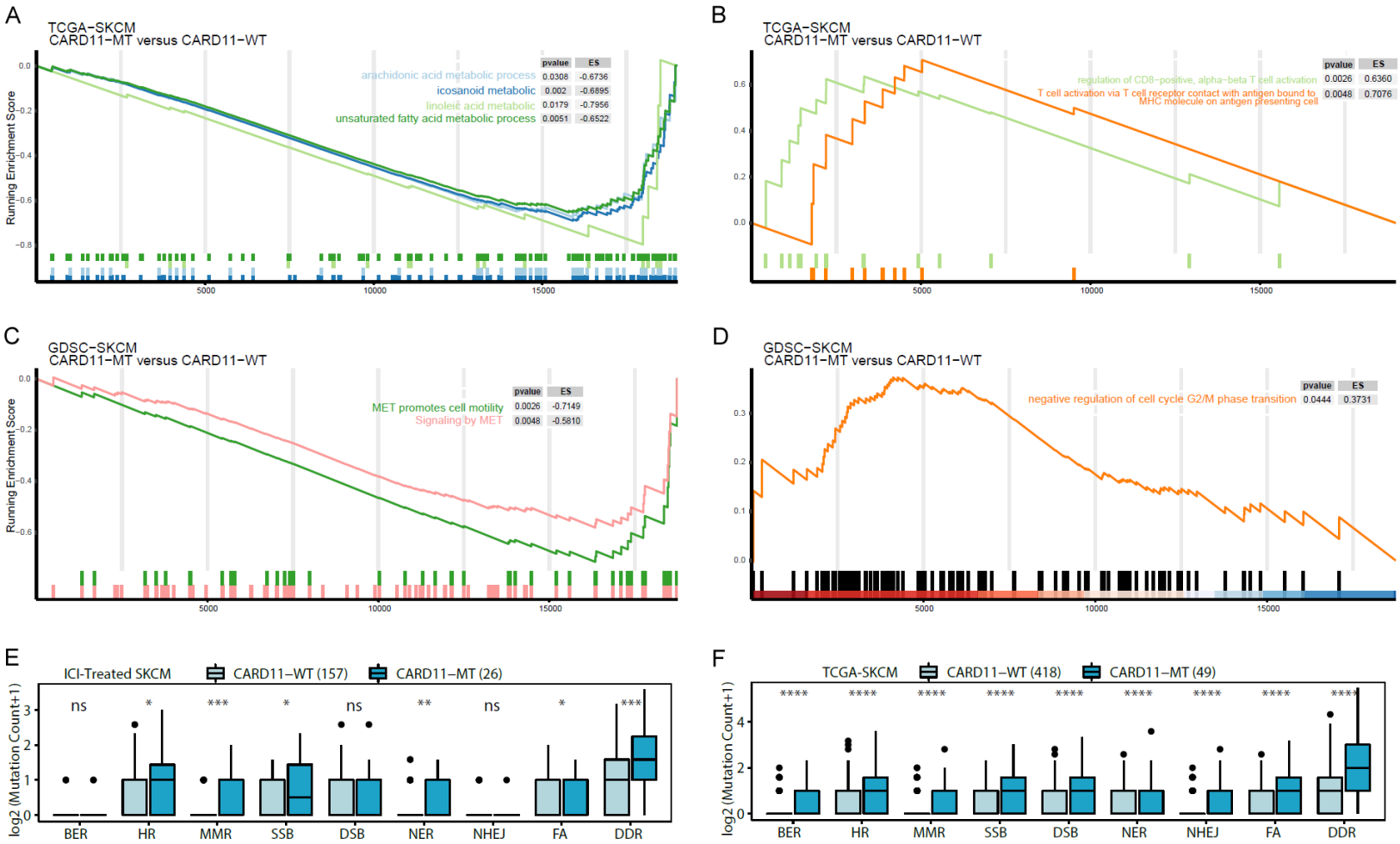

Figure 4. Analysis of CARD11 mutation-related pathways. A-D. Gene set enrichment analysis related to the improved CARD11-MT prognosis. Enrichment results for gene pathways that were significantly upregulated or downregulated in CARD11-MT tumors are shown. Significance was defined as $P < 0.05$. E, F. Comparison of the number of DDR pathway mutations between CARD11-MT and CARD11-WT tumors in the SKCM immunotherapy cohort and TCGA-SKCM cohort.

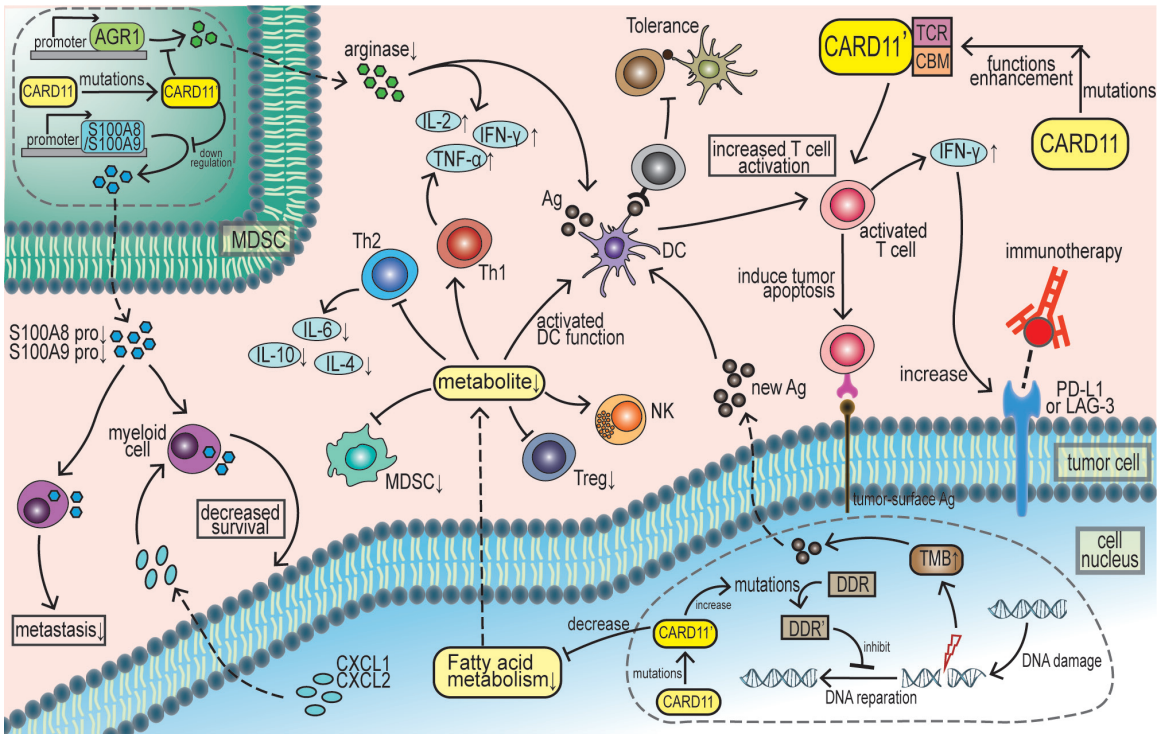

Figure 5. Possible mechanisms for the improved prognosis after immunotherapy of CARD11-MT patients. (1) Mechanisms related to fatty acid metabolism: In CARD11-MT tumors, fatty acid metabolism-related pathways are significantly downregulated. The secretion of fatty acid metabolites by tumor cells into the immune microenvironment is reduced, which can relieve the original immunosuppression and activate antitumor immunity in the following ways: (a) promoting the proliferation and activity of CD8+ T cells; (b) promoting the antitumor activity of natural killer cells; (c) inhibiting the proliferation of Tregs and MDSCs; and (d) enhancing the ability of tumor cells to present tumor antigens and promoting the differentiation and function of dendritic cells. (2) Downregulation of MDSC gene expression: ARG1 expression products have immunosuppressive effects. The reduction in ARG1 expression product levels promotes T cell regeneration and activation while increasing the secretion of cytokines such as IFN-γ, TNF-α, and IL-2. ARG1 downregulation also results in weakened MDSC function in the tumor immune microenvironment. Therefore, the inhibition of T cell activation and IFN-γ is attenuated. (3) Upregulation of T cell activation: T cells are important cells in antitumor immunity. As the number of activated T cells in the TME increases, immune checkpoint inhibitor treatment becomes more effective. (4) Increase in the number of DDR pathway mutations: Increasing the number of DDR pathway gene mutations increases the TMB and NAL significantly, which can promote T cell activation and the recognition of tumor antigens. The expression of some immune factors, such as immune checkpoints (PD-L1 and LAG3) and IFNγ, also increases as the number of DDR pathway mutations increases. Therefore, CARD11-MT tumors are more immunogenic and more sensitive to immunotherapy than CARD11-WT tumors.

CoA (CoA), have recently been shown to be closely related to tumor development [29].

Additionally, we found that T cell activation signaling pathways were significantly enriched in CARD11-MT patients. ICIs, such as PD-L1 blockers, exert antitumor effects by binding to immune checkpoints on the surface of tumor cells (such as PD-L1); therefore, T cells can then recognize tumor cells. Thus, ICI treatments require a sufficient number of activated CD8+ T cells. Existing studies have shown that CARD11 can activate TCR in the downstream pathway of the CARD11 gene, and CBM as well as TCR are essential components of antigen-induced T cell activation [30]. Correspondingly, we found through GSEA that T cell activation signaling pathways were significantly upregulated in CARD11-MT tumors, which may be caused by mutant CARD11 having an enhanced function. As a consequence, the number of activated T cells will increase, and ICI treatment will be more effective.

Finally, by analyzing the number of DDR pathway mutations in the immunotherapy cohort and TCGA-SKCM cohort, we found that CARD 11-MT tumors had a higher number of muta-

tions than CARD11-WT tumors. Recent studies [31] have shown that as the number of DDR pathway mutations increases, the TMB and NAL significantly increase. There are potential interactions between different DDR pathways. Patients with specific DDR comutations show a higher TMB and NAL than others, and immunomodulatory factors, such as immune checkpoints (PD- L1 and LAG3) and IFNγ, also show relatively high mRNA expression levels. These factors can ultimately activate the antitumor immune response more effectively and improve the efficacy of ICIs. In addition, IFN-γ secreted by antitumor immune cells can upregulate the expression of immune checkpoint molecules, such as PD-L1 and LAG3, on the surface of tumor cells, which can enhance the efficacy of ICI therapy in the context of normal T cell function [32].

Results of previous research indicate that the expression of CARD11 can predict the prognosis of patients with diffuse large B-cell lymphoma (DLBCL), and the positive expression of CARD11 is significantly associated with lower event-free survival (EFS) in patients with DLBCL [33]. The activation of the NF-κB pathway induced by antigen receptors requires the expression product of CARD11 in normal B cells, and the overexpression of CARD11 can lead to excessive activation of the NF-κB pathway [34, 35]. NF-κB activation is very common in cancer. In all malignant tumors, NF-κB acts in a cell-type specific way: activates pro-inflammatory genes in tumor microenvironment (TME) components, such as IL-1, IL-6, reactive oxygen, etc [36]. These cytokines form an immunosuppressive microenvironment, thereby promoting tumor growth and metastasis. We speculate that the CARD11 mutation we detected in SKCM may be located in an important functional area. The CARD11 mutation in SKCM inhibits the original function of CARD11, which has the opposite effect to the CARD11 mutation in DLBCL and promotes the development and invasion of SKCM, leading to a low survival rate in patients. In the future, we need to conduct more experiments to test this hypothesis.

At present, there are still some SKCM patients who experience failed anti-PD1/PDL1 treatment or drug resistance [37]. Several recent clinical trials have shown that the use of CTLA-4 monoclonal antibody [38], immunotherapy combined with targeted therapy [39], and anti-PD-1 combined with T-Vec oncolytic virus therapy [40] may improve the clinical prognosis of drug-resistant patients. Therefore, the main challenge for SKCM immunotherapy is to understand the immunobiology of tumors with primary or acquired resistance to immunotherapy and to develop effective immunotherapy for specific subtypes as well as strive for long-term clinical benefits [41]. In the process of immunotherapy, cells in the TME (such as activated T lymphocytes) and cytokines (such as IFN-γ) play a significant role. Therefore, the development of predictive biomarkers related to the TME can help us to have a deeper understanding of the mechanism of SKCM immunotherapy failure. Previous studies have shown that the targeting CBM complex can activate Tregs to produce IFN-γ [7], simulating the anti-tumor immunity for immune checkpoint therapy. This suggests that drugs targeting CARD11 and its downstream pathways may assist immunotherapy and make ICIs produce longer-lasting therapeutic effects. A previous clinical trial showed that CARD11 mutations may affect the response of lymphoma patients to ibrutinib. CARD11 may be used as a biomarker to evaluate the therapeutic effect of BTK inhibitors in the treatment of early lymphoma patients and inform clinical decisions.

In summary, we found that the CARD11 gene can be used as a marker for predicting the efficacy of ICI treatments in SKCM patients. By grouping patients by the CARD11 mutational status, we can distinguish the prognosis of SKCM patients after immunotherapy. We explained the relationship between CARD11 gene mutation and the tumor immune microenvironment through bioinformatic analysis and further discussed and summarized some molecular mechanisms of CARD11 gene mutation affecting the efficacy of ICI therapy. However, as a retrospective study, this study has some limitations. Our sample size is small, and there is no prospective study to further validate our conclusions. Moreover, the mechanism of CARD11 gene mutation leading to the downregulation of the fatty acid metabolism pathway and MDSC gene expression has not been elucidated. In the future, to improve specificity and sensitivity, we can combine CARD11 gene mutations with other predictive biomarkers of ICI therapy, such as the TMB and PD-1 expression,

and ultimately accurately screen patients to identify those who will have a long-term effective response to ICI treatment.

Disclosure of conflict of interest

None.

Address correspondence to: Jian Zhang and Peng Luo, Department of Oncology, Zhujiang Hospital, Southern Medical University, 253 Industrial Avenue, Guangzhou 510282, Guangdong, China. Tel: +86-13925091863; Fax: +86-020-61643888; E-mail: blacktiger@139.com (JZ); luopeng@smu.edu.cn (PL)

References

[1] Chinese guidelines for diagnosis and treatment of melanoma 2018 (English version). Chin J Cancer Res 2019; 31: 578-585.

[2] Chapman PB, Hauschild A, Robert C, Haanen JB, Ascierto P, Larkin J, Dummer R, Garbe C, Testori A, Maio M, Hogg D, Lorigan P, Lebbe C, Jouary T, Schadendorf D, Ribas A, O'Day SJ, Sosman JA, Kirkwood JM, Eggermont AM, Dreno B, Nolop K, Li J, Nelson B, Hou J, Lee RJ, Flaherty KT and McArthur GA. Improved survival with vemurafenib in melanoma with BRAF V600E mutation. N Engl J Med 2011; 364: 2507-2516.

[3] Levine O, Devji T and Xie F. Systemic therapy for previously untreated advanced BRAF-mutated melanoma: navigating a shifting landscape. Immunotherapy 2017; 9: 375-378.

[4] Johnson DB, Lovly CM, Sullivan RJ, Carvajal RD and Sosman JA. Melanoma driver mutations and immune therapy. Oncoimmunology 2016; 5: e1051299.

[5] Johnson DB, Frampton GM, Rioth MJ, Yusko E, Xu Y, Guo X, Ennis RC, Fabrizio D, Chalmers ZR, Greenbowe J, Ali SM, Balasubramanian S, Sun JX, He Y, Frederick DT, Puzanov I, Balko JM, Cates JM, Ross JS, Sanders C, Robins H, Shyr Y, Miller VA, Stephens PJ, Sullivan RJ, Sosman JA and Lovly CM. Targeted next generation sequencing identifies markers of response to PD-1 blockade. Cancer Immunol Res 2016; 4: 959-967.

[6] Bedsaul JR, Carter NM, Deibel KE, Hutcherson SM, Jones TA, Wang Z, Yang C, Yang YK and Pomerantz JL. Mechanisms of regulated and dysregulated CARD11 signaling in adaptive immunity and disease. Front Immunol 2018; 9: 2105.

[7] Rosenbaum M, Gewies A, Pechloff K, Heuser C, Engleitner T, Gehring T, Hartjes L, Krebs S, Krappmann D, Kriegsmann M, Weichert W, Rad R, Kurts C and Ruland J. Bcl10-controlled Malt1 paracaspase activity is key for the immune suppressive function of regulatory T cells. Nat Commun 2019; 10: 2352.

[8] Samstein RM, Lee CH, Shoushtari AN, Hellmann MD, Shen R, Janjigian YY, Barron DA, Zehir A, Jordan EJ, Omuro A, Kaley TJ, Kendall SM, Motzer RJ, Hakimi AA, Voss MH, Russo P, Rosenberg J, Iyer G, Bochner BH, Bajorin DF, Al-Ahmadie HA, Chaft JE, Rudin CM, Riely GJ, Baxi S, Ho AL, Wong RJ, Pfister DG, Wolchok JD, Barker CA, Gutin PH, Brennan CW, Tabar V, Mellinghoff IK, DeAngelis LM, Ariyan CE, Lee N, Tap WD, Gounder MM, D'Angelo SP, Saltz L, Stadler ZK, Scher HI, Baselga J, Razavi P, Klebanoff CA, Yaeger R, Segal NH, Ku GY, DeMatteo RP, Ladanyi M, Rizvi NA, Berger MF, Riaz N, Solit DB, Chan TA and Morris LGT. Tumor mutational load predicts survival after immunotherapy across multiple cancer types. Nat Genet 2019; 51: 202-206.

[9] Colaprico A, Silva TC, Olsen C, Garofano L, Cava C, Garolini D, Sabedot TS, Malta TM, Pagnotta SM, Castiglioni I, Ceccarelli M, Bontempi G and Noushmehr H. TCGAbiolinks: an R/Bioconductor package for integrative analysis of TCGA data. Nucleic Acids Res 2016; 44: e71.

[10] Cerami E, Gao J, Dogrusoz U, Gross BE, Sumer SO, Aksoy BA, Jacobsen A, Byrne CJ, Heuer ML, Larsson E, Antipin Y, Reva B, Goldberg AP, Sander C and Schultz N. The cBio cancer genomics portal: an open platform for exploring multidimensional cancer genomics data. Cancer Discov 2012; 2: 401-404.

[11] Thorsson V, Gibbs DL, Brown SD, Wolf D, Bortone DS, Ou Yang TH, Porta-Pardo E, Gao GF, Plaisier CL, Eddy JA, Ziv E, Culhane AC, Paull EO, Sivakumar IKA, Gentles AJ, Malhotra R, Farshidfar F, Colaprico A, Parker JS, Mose LE, Vo NS, Liu J, Liu Y, Rader J, Dhankani V, Reynolds SM, Bowlby R, Califano A, Cherniack AD, Anastassiou D, Bedognetti D, Mokrab Y, Newman AM, Rao A, Chen K, Krasnitz A, Hu H, Malta TM, Noushmehr H, Pedamallu CS, Bullman S, Ojesina AI, Lamb A, Zhou W, Shen H, Choueiri TK, Weinstein JN, Guinney J, Saltz J, Holt RA, Rabkin CS, Lazar AJ, Serody JS, Demicco EG, Disis ML, Vincent BG and Shmulevich I. The immune landscape of cancer. Immunity 2018; 48: 812-830, e814.

[12] Yang W, Soares J, Greninger P, Edelman EJ, Lightfoot H, Forbes S, Bindal N, Beare D, Smith JA, Thompson IR, Ramaswamy S, Futreal PA, Haber DA, Stratton MR, Benes C, McDermott U and Garnett MJ. Genomics of Drug Sensitivity in Cancer (GDSC): a resource for therapeutic biomarker discovery in cancer cells. Nucleic Acids Res 2013; 41: D955-961.

[13] Chalmers ZR, Connelly CF, Fabrizio D, Gay L, Ali SM, Ennis R, Schrock A, Campbell B, Shlien A,

Chmielecki J, Huang F, He Y, Sun J, Tabori U, Kennedy M, Lieber DS, Roels S, White J, Otto GA, Ross JS, Garraway L, Miller VA, Stephens PJ and Frampton GM. Analysis of 100,000 human cancer genomes reveals the landscape of tumor mutational burden. Genome Med 2017; 9: 34.

[14] Gu Z, Eils R and Schlesner M. Complex heatmaps reveal patterns and correlations in multidimensional genomic data. Bioinformatics 2016; 32: 2847-2849.

[15] Mayakonda A, Lin DC, Assenov Y, Plass C and Koeffler HP. Maftools: efficient and comprehensive analysis of somatic variants in cancer. Genome Res 2018; 28: 1747-1756.

[16] Newman AM, Liu CL, Green MR, Gentles AJ, Feng W, Xu Y, Hoang CD, Diehn M and Alizadeh AA. Robust enumeration of cell subsets from tissue expression profiles. Nat Methods 2015; 12: 453-457.

[17] Hao D, Liu J, Chen M, Li J, Wang L, Li X, Zhao Q and Di LJ. Immunogenomic analyses of advanced serous ovarian cancer reveal immune score is a strong prognostic factor and an indicator of chemosensitivity. Clin Cancer Res 2018; 24: 3560-3571.

[18] Reich M, Liefeld T, Gould J, Lerner J, Tamayo P and Mesirov JP. GenePattern 2.0. Nat Genet 2006; 38: 500-501.

[19] Robinson MD, McCarthy DJ and Smyth GK. edgeR: a Bioconductor package for differential expression analysis of digital gene expression data. Bioinformatics 2010; 26: 139-140.

[20] Yu G, Wang LG, Han Y and He QY. clusterProfiler: an R package for comparing biological themes among gene clusters. Omics 2012; 16: 284-287.

[21] Subramanian A, Tamayo P, Mootha VK, Mukherjee S, Ebert BL, Gillette MA, Paulovich A, Pomeroy SL, Golub TR, Lander ES and Mesirov JP. Gene set enrichment analysis: a knowledge-based approach for interpreting genome-wide expression profiles. Proc Natl Acad Sci U S A 2005; 102: 15545-15550.

[22] Kassambara, A. (2018): ggpubr: 'ggplot2' Based Publication Ready Plots. R package version 0.1.7. Available at: https://CRAN.R-project.org/package=ggpubr.

[23] Draghiciu O, Lubbers J, Nijman HW and Daemen T. Myeloid derived suppressor cells-An overview of combat strategies to increase immunotherapy efficacy. Oncoimmunology 2015; 4: e954829.

[24] Munder M, Schneider H, Luckner C, Giese T, Langhans CD, Fuentes JM, Kropf P, Mueller I, Kolb A, Modolell M and Ho AD. Suppression of T-cell functions by human granulocyte arginase. Blood 2006; 108: 1627-1634.

[25] Bresnick AR, Weber DJ and Zimmer DB. S100 proteins in cancer. Nat Rev Cancer 2015; 15: 96-109.

[26] Medes G, Thomas A and Weinhouse S. Metabolism of neoplastic tissue. IV. A study of lipid synthesis in neoplastic tissue slices in vitro. Cancer Res 1953; 13: 27-29.

[27] Sheng H, Shao J, Morrow JD, Beauchamp RD and DuBois RN. Modulation of apoptosis and Bcl-2 expression by prostaglandin E2 in human colon cancer cells. Cancer Res 1998; 58: 362-366.

[28] Röhrig F and Schulze A. The multifaceted roles of fatty acid synthesis in cancer. Nat Rev Cancer 2016; 16: 732-749.

[29] Luo X, Cheng C, Tan Z, Li N, Tang M, Yang L and Cao Y. Emerging roles of lipid metabolism in cancer metastasis. Mol Cancer 2017; 16: 76.

[30] Gehring T, Erdmann T, Rahm M, Graß C, Flatley A, O'Neill TJ, Woods S, Meininger I, Karayel O, Kutzner K, Grau M, Shinohara H, Lammens K, Feederle R, Hauck SM, Lenz G and Krappmann D. MALT1 phosphorylation controls activation of T lymphocytes and survival of ABC-DLBCL tumor cells. Cell Rep 2019; 29: 873-888, e810.

[31] Wang Z, Zhao J, Wang G, Zhang F, Zhang Z, Zhang F, Zhang Y, Dong H, Zhao X, Duan J, Bai H, Tian Y, Wan R, Han M, Cao Y, Xiong L, Liu L, Wang S, Cai S, Mok TSK and Wang J. Comutations in DNA damage response pathways serve as potential biomarkers for immune checkpoint blockade. Cancer Res 2018; 78: 6486-6496.

[32] Abiko K, Matsumura N, Hamanishi J, Horikawa N, Murakami R, Yamaguchi K, Yoshioka Y, Baba T, Konishi I and Mandai M. IFN-γ from lymphocytes induces PD-L1 expression and promotes progression of ovarian cancer. Br J Cancer 2015; 112: 1501-1509.

[33] Zhao D, Li D, Zhong D and Zhang W. Expression and prognostic value of CARD11 in diffuse large B cell lymphoma. Zhonghua Xue Ye Xue Za Zhi 2016; 37: 30-34.

[34] Lenz G, Davis RE, Ngo VN, Lam L, George TC, Wright GW, Dave SS, Zhao H, Xu W, Rosenwald A, Ott G, Muller-Hermelink HK, Gascoyne RD, Connors JM, Rimsza LM, Campo E, Jaffe ES, Delabie J, Smeland EB, Fisher RI, Chan WC and Staudt LM. Oncogenic CARD11 mutations in human diffuse large B cell lymphoma. Science 2008; 319: 1676-1679.

[35] Davis RE, Brown KD, Siebenlist U and Staudt LM. Constitutive nuclear factor kappaB activity is required for survival of activated B cell-like diffuse large B cell lymphoma cells. J Exp Med 2001; 194: 1861-1874.

[36] DiDonato JA, Mercurio F and Karin M. NF-κB and the link between inflammation and cancer. Immunol Rev 2012; 246: 379-400.

[37] Weiss SA, Wolchok JD and Sznol M. Immunotherapy of melanoma: facts and hopes. Clin Cancer Res 2019; 25: 5191-5201.
[38] Larkin J, Chiarion-Sileni V, Gonzalez R, Grob JJ, Rutkowski P, Lao CD, Cowey CL, Schadendorf D, Wagstaff J, Dummer R, Ferrucci PF, Smylie M, Hogg D, Hill A, Márquez-Rodas I, Haanen J, Guidoboni M, Maio M, Schöffski P, Carlino MS, Lebbé C, McArthur G, Ascierto PA, Daniels GA and Long GV. Five-year survival with combined nivolumab and ipilimumab in advanced melanoma. N Engl J Med 2019; 381: 1535-1546.
[39] Long GV, Weber JS, Infante JR, Kim KB, Daud A, Gonzalez R, Sosman JA, Hamid O, Schuchter L, Cebon J, Kefford RF, Lawrence D, Kudchadkar R, Burris HA 3rd, Falchook GS, Algazi A, Lewis K, Puzanov I, Ibrahim N, Sun P, Cunningham E, Kline AS, Del Buono H, McDowell DO, Patel K and Flaherty KT. Overall survival and durable responses in patients With BRAF V600-mutant metastatic melanoma receiving dabrafenib combined with trametinib. J Clin Oncol 2016; 34: 871-878.
[40] Bommareddy PK, Patel A, Hossain S and Kaufman HL. Talimogene Laherparepvec (T-VEC) and other oncolytic viruses for the treatment of melanoma. Am J Clin Dermatol 2017; 18: 1-15.
[41] Franklin C, Livingstone E, Roesch A, Schilling B and Schadendorf D. Immunotherapy in melanoma: recent advances and future directions. Eur J Surg Oncol 2017; 43: 604-611.

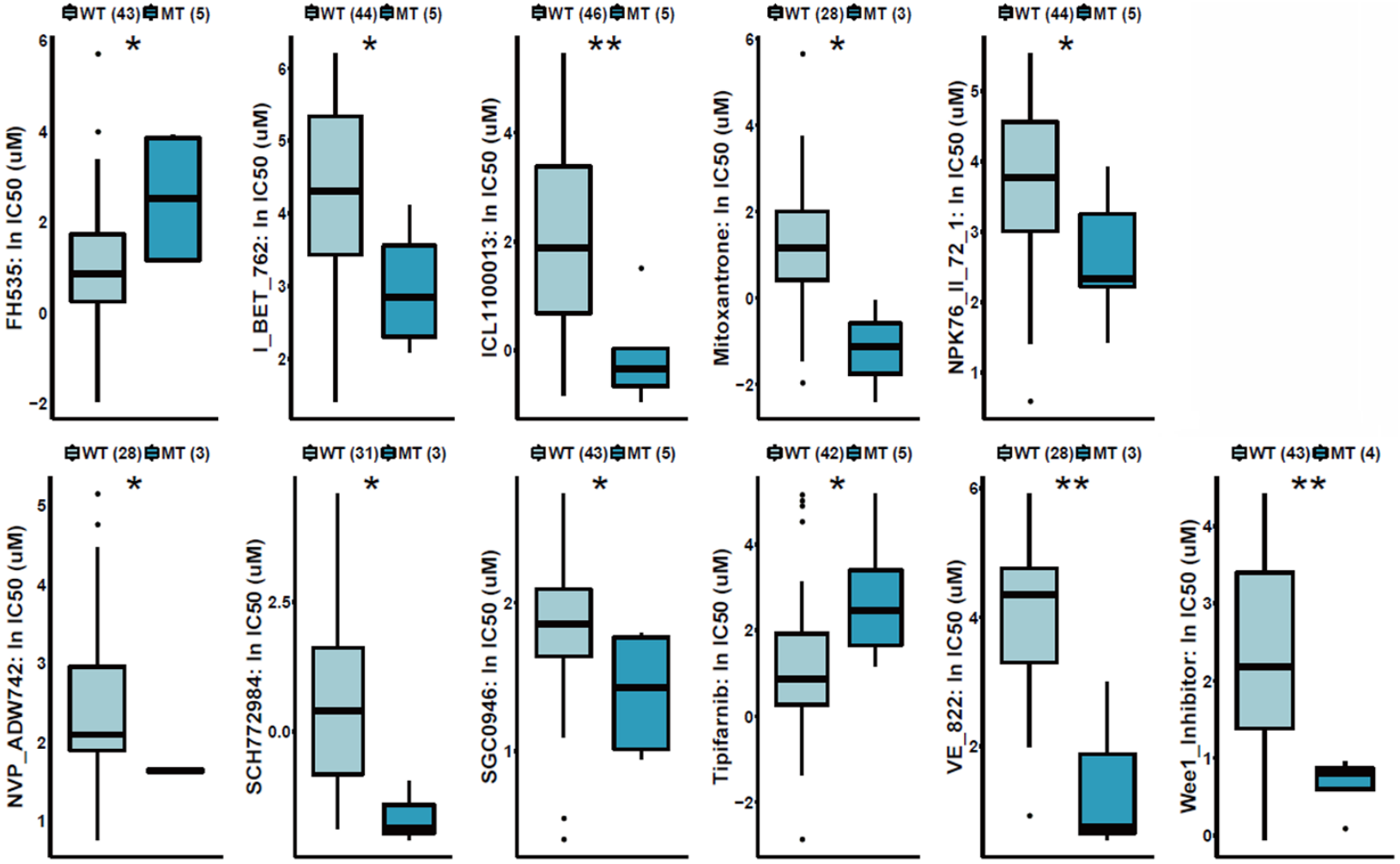

Figure S1. Significant differences in SKCM tumor cell drug sensitivity were analyzed. SKCM cell lines drug sensitivity data were downloaded from GDSC and used to determine the drug sensitivity differences between CARD11-WT and CARD11-MT tumors.

Table S1. List of genes included in DNA damage response (DDR) gene set used for comparison analysis (MsiDB)

DNA damage response (DDR) gene set	List of genes
BER(R-HSA-73884_REACTOME_Base_Excision_Repair)	CCNO, POLD3, FEN1, SMUG1, APEX1, LIG1, LIG3, MPG, MUTYH, NTHL1, OGG1, PCNA, POLB, POLD1, POLD2, POLD4, TDG, XRCC1, MBD4
DSB(R-HAS-5696398_REACTOME_Double_Strand_Break_Repair)	RAD50, XRCC6, H2AFX, LOC389901, LIG1, LIG4, MRE11A, NBN, ATM, TDP1, PRKDC, RAD51, RAD52, RPA1, RPA2, RPA3, LOC651610, BRCA1, BRCA2, TP53BP1, XRCC4, XRCC5, BRIP1, MDC1
FA(R-HAS-6783310_REACTOME_Fanconi_Anemia_Pathway)	FANCA, FANCC, FANCD2, FANCE, FANCB, FANCF, FANCG, ZBTB32, UBE2T, ATM, ATR, FANCL, FANCM, RPS27A, LOC648152, LOC651610, LOC651921, BRCA1, BRCA2, RPS27AP11, UBA52, RPS27AP11, USP1, PALB2, C17orf70, C19orf40
HR(hsa03440_KEGG_ Homologous_Recombination)	RAD50, H2AFX, LIG1, MRE11A, NBN, ATM, RAD51, RAD52, RPA1, RPA2, RPA3, LOC651610, BRCA1, BRCA2, TP53BP1, BRIP1, MDC1, RAD50, POLD3, EME1, RAD54B, RPA4, MRE11A, NBN, POLD1, POLD2, POLD4, RAD51, RAD51C, RAD51B, RAD51D, RAD52, RPA1, RPA2, RPA3, BLM, SSBP1, BRCA2, TOP3A, XRCC2, XRCC3, SHFM1, MUS81, RAD54 L, TOP3B
MMR(hsa03430_KEGG_Mismatch_Repair)	POLD3, MLH3, MSH6, RPA4, LIG1, MLH1, MSH2, MSH3, PCNA, PMS2, POLD1, POLD2, POLD4, RFC1, RFC2, RFC3, RFC4, RFC5, RPA1, RPA2, RPA3, SSBP1, EX01
NER(R-HSA-5696398_REACTOME_Nucleotide_Excision_Repair)	CDK7, POLD3, ERCC8, DDB1, DDB2, ERCC1, ERCC2, ERCC3, ERCC4, ERCC5, ERCC6, GTF2H1, GTF2H2, GTF2H3, GTF2H4, LIG1, MNAT1, PCNA, POLD1, POLD2, POLE, POLE2, POLR2A, POLR2B, POLR2C, POLR2D, POLR2E, POLR2F, POLR2G, POLR2H, POLR2I, POLR2J, POLR2K, POLR2 L, XAB2, POLD4, RAD23B, RFC2, RFC3, RFC4, RFC5, RPA1, RPA2, RPA3, LOC652672, LOC652857, GTF2H2B, TCEA1, XPA, XPC, CCNH
NHEJ(hsa03450_KEGG_Non_Homologous_End_Joining)	RAD50, DNTT, FEN1, XRCC6, POLL, POLM, LIG4, MRE11A, PRKDC, DCLRE1C, LOC731751, XRCC4, XRCC5, NHEJ1
SSB(GO:0003697_Single_Stranded_DNA_Binding)	ERCC1, ERCC4, ERCC5, FUBP1, HMGB2, HNRNPA1, HNRNPA2B1, HNRPDL, IGHMBP2, MLH1, MSH2, MSH3, MYT2, PCBP1, PMS2, POT1, PURA, PURB, RAD23A, RAD23B, RAD51, RAD51AP1, RBMS1, RPA1, RPA2, RPA3, RPA4, SUB1, TERF2, TERF2IP, TP53, TREX1, WBP11, XPC, YBX1
DDR(merged)	CCNO, POLD3, FEN1, SMUG1, APEX1, LIG1, LIG3, MPG, MUTYH, NTHL1, OGG1, PCNA, POLB, POLD1, POLD2, POLD4, TDG, XRCC1, MBD4, TCEA1, ERCC8, LOC652857, RPA3, RPA3, DDB2, POLR2E, POLR2H, RFC2, XPA, RFC3, ERCC1, RPA2, RPA2, CCNH, XAB2, ERCC6, POLE, ERCC2, RAD23B, POLR2J, POLR2G, DDB1, ERCC5, RPA1, RPA1, LOC652672, GTF2H2, POLR2B, ERCC4, POLR2 L, POLR2A, RFC4, GTF2H1, ERCC3, RFC5, GTF2H4, GTF2H2B, POLR2D, POLR2I, CDK7, GTF2H3, POLE2, XPC, POLR2C, MNAT1, POLR2K, POLR2F, MSH3, MSH2, SSBP1, RFC1, EX01, MLH1, RPA4, PMS2, MSH6, MLH3, PCBP1, PURB, ERCC1, HMGB2, IGHMBP2, RBMS1, RAD23B, HNRNPA2B1, TP53, ERCC5, TERF2IP, PURA, TREX1, ERCC4, WBP11, POT1, RAD51AP1, MYT2, RAD23A, HNRPDL, XPC, FUBP1, RAD51, RAD51, SUB1, HNRNPA1, YBX1, TERF2, RAD50, RAD50, H2AFX, LIG4, PRKDC, XRCC4, LOC651610, NBN, NBN, XRCC6, BRIP1, RAD52, RAD52, TP53BP1, BRCA1, MRE11A, MRE11A, MDC1, TDP1, LIG1, BRCA2, BRCA2, LOC389901, ATM, XRCC5, RAD54 L, SHFM1, POLD3, TOP3A, XRCC3, POLD4, RAD51B, SSBP1, TOP3B, RAD51D, MUS81, POLD1, EME1, RPA4, RAD54B, RAD51C, XRCC2, BLM, POLD2, LIG4, PRKDC, NHEJ1, XRCC4, FEN1, POLM, XRCC6, DNTT, LOC731751, POLL, DCLRE1C, XRCC5, FANCA, FANCC, FANCD2, FANCE, FANCB, FANCF, FANCG, ZBTB32, UBE2T, ATM, ATR, FANCL, FANCM, RPS27A, LOC648152, LOC651610, LOC651921, BRCA1, BRCA2, RPS27AP11, UBA52, RPS27AP11, USP1, PALB2, C17orf70, C19orf40